Decoupling Planarizing and Steric Energetics to Accurately Model the Rigidity of π-Conjugated Polymers

Andrew T. Kleinschmidt, Alexander X. Chen, Robert S. Ramji, Tod A. Pascal,* and Darren J. Lipomi*

Cite This: https://doi.org/10.1021/acs.jpcb.2c08843

Read Online

ACCESS | Metrics & More | Article Recommendations | Supporting Information

ABSTRACT: The π-conjugated backbone of semiconducting polymers gives rise to both their electronic properties and structural rigidity. However, current computational methods for understanding the rigidity of polymer chains fail in one crucial way. Namely, standard torsional scan (TS) methods do not satisfactorily capture the behavior of polymers exhibiting a high degree of steric hindrance. This deficiency in part stems from the method by which torsional scans decouple energy related to electron delocalization from that related to nonbonded interactions. These methods do so by applying classical corrections of the nonbonded energy to the quantum mechanical (QM) torsional profile for polymers that are highly sterically hindered. These large corrections to the energy from nonbonded interactions can substantially skew the calculated QM energies related to torsion, resulting in an inaccurate or imprecise estimation of the rigidity of a polymer. As a consequence, simulations of the morphology of a highly sterically hindered polymer using the TS method can be highly inaccurate. Here, we describe an alternative, generalizable method by which the delocalization energy can be decoupled from the energy associated with nonbonded interactions—the "isolation of delocalization energy" (DE) method. From torsional energy calculations, we find that the relative accuracy of the DE method is similar to the TS method (within 1 kJ/mol) for two model polymers (P3HT, PTB7) when compared to quantum mechanical calculations. However, the DE method significantly increased the relative accuracy for simulations of PNDI-T, a highly sterically hindered polymer (8.16 kJ/mol). Likewise, we show that comparison of the planarization energy (i.e., backbone rigidity) from torsional parameters is significantly more precise for both PTB7 and PNDI-T when using the DE method as opposed to the TS method. These differences affect the simulated morphology, with the DE method predicting a significantly more planar configuration of PNDI-T.
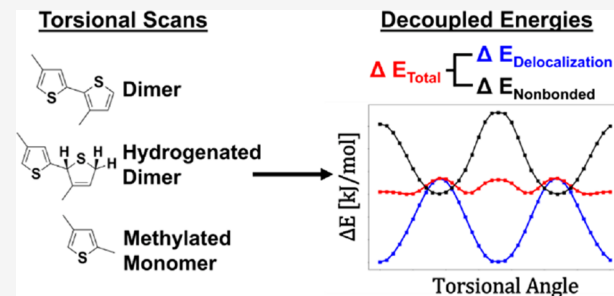
INTRODUCTION

The backbone structures of π-conjugated polymers differ dramatically from those of polymers with saturated backbones. These polymeric semiconductors are generally composed of a backbone consisting of aromatic and/or heteroaromatic rings bonded to one another.[1,2] Charge transport in these conjugated structures is enabled by delocalization between overlapping π-orbitals,[3−5] which gives rise to the band structure.[6] Electronic delocalization is generally energetically favorable, resulting in highly planar polymer chains.[7−9] The semiconducting behavior of these π-conjugated materials in particular has given rise to a myriad of device applications, from organic transistors[10] and solar cells[11] to chemical sensors.[12] Due to their mechanical robustness and synthetic tunability, organic electronic devices fabricated from conjugated polymers have many advantages over their inorganic counterparts. In particular, polymers with the "donor–acceptor" motif—in which electron-rich and electron-poor monomer residues alternate along the backbone—can achieve low bandgaps and high mobilities. Furthermore, this "push–pull" effect further drives coplanarity of adjacent monomers in donor–acceptor polymers.[13,14]

Electronic delocalization between adjacent monomers is thus a defining characteristic of conjugated polymers.[15,16] Computational modeling of conjugated polymers potentially offers a high-throughput method of analyzing relationships between the structure of the individual chains and the morphology in the solid state. In such models, the ability to predict the rigidity of the backbone depends on accurate determination of the energy of electronic delocalization between adjacent monomers, a task that is not trivial. Typically, the energy is calculated by means of the torsional scan (TS) method, in which the torsional angle between adjacent monomers is steadily adjusted and the total energy is calculated through a quantum mechanical (QM) method at each torsional value.[17,18] The total QM energy is then modified

by the nonbonded energy, as calculated by a force field, to yield data points to which dihedral parameters are fitted. Typically, simulations using the OPLS (Optimized Potentials for Liquid Simulations) force field use the 12−6 Lennard-Jones formulation for van der Waals interactions as well as a Coulombic term for electrostatic interactions to describe nonbonded forces between atoms. This TS method has become standard to model and understand the rigidity of conjugated polymers.[19−21] However, the nonbonded energy calculated by the TS method nearly always increases at planarity due to steric clashes between atoms brought into close proximity (i.e., as in the eclipsed conformation in a Newman projection). Thus, nonbonded energy acts to counter (and sometimes overwhelm) the favorable energy of electron delocalization. The aforementioned determination of non-bonded energy causes the calculated energy of simulated structures to increase quickly at small interatomic distances. When a chemical structure has significant steric clashes during a torsional scan, this large nonbonded term can intractably skew the data used by this conventional method to fit dihedral parameters, rendering the resulting parameters inaccurate. Yet, highly sterically hindered and twisted polymers have become increasingly common in organic electronics, particularly in experimental studies. Thus, a need arises to ensure that the polymers commonly used for device applications can be accurately modeled.

Other work has focused on improving the accuracy and applicability of OPLS force fields to conjugated polymers by accounting for nonbonded interactions in different ways.[18,21−26] For example, Jackson et al. employed a more accurate method (developed by DuBay et al.[21]) for fitting OPLS dihedral parameters to a diverse library of conjugated polymers. The authors minimized steric interactions by first optimizing the geometry of the dimer at the QM level. Then, the electrostatic interactions were defined for the optimized geometric configuration using a B3LYP/6-31+G** CHelpG calculation, thus assigning point charges to the donor and acceptor moieties for each conjugated polymer. Next, the authors performed a QM torsional scan at the MP2 level to produce a profile for the intermonomer dihedral potentials. Because the QM torsional scan includes nonbonded interactions, which are independently accounted for in the OPLS force field, the nonbonded component must be separated from the QM torsional profile before OPLS dihedral parameters can be fit. To avoid double counting the nonbonded energy in the dihedral parameters, an additional torsional scan was performed to calculate the isolated energy of the nonbonded interactions (i.e., electrostatics, van der Waals, and steric interactions) using the OPLS force field. The energies from this scan were subtracted from the energies of the QM scan, and the resulting data were used in the dihedral fitting procedure. This modified torsional scan method was highly accurate for 15 diverse chemical structures simulated. However, steric hindrance remained a problem. When this method was applied to a conjugated polymer species with close steric contacts at planarity, the point charges and van der Waals interactions resulted in large errors when rotating the monomer across the torsional potentials (relative to the quantum mechanical results), rendering the resulting dihedral parameters inaccurate.[18] Additional work has been conducted to more accurately determine the effects of nonbonded interactions and electron delocalization on polymer conforma-tions. Thorley and McCulloch used functional group intra-

molecular symmetry adapted perturbation theory (FI-SAPT) to examine nonbonded inter-ring interactions (e.g., S···F and S···O) and their effects on torsional profiles.[27] The study elucidated the role of these nonbonded interactions as stabilizing forces within a conjugated backbone. In particular, the findings suggest that the addition of S···F and S···O interactions can provide both stabilizing and destabilizing forces, as molecular structure affects the energies related to nonbonded interactions, electrostatics, and delocalization. Che and Perepichka performed torsional scans on the bond bridging adjacent aromatic structures in order to elucidate the effect of bond lengths and chemical structure of the backbone.[28] The authors propose the average squared cosine ($\langle \cos^2 \varphi \rangle$), where φ is the torsional angle, as a representation of planarity and orbital overlap. The findings suggest that $\langle \cos^2 \varphi \rangle$ is a good predictor of backbone planarity, as affected by steric repulsion, electrostatic interactions, donor−acceptor interactions, conjugation length, and delocalization due to aromatic structures. Finally, Karunasena et al. used atoms-in-molecules (AIM) analysis and MD simulations to more accurately determine the role of nonbonded interactions (e.g., N···H, F···H, S···F, and S···N) on polymer conformation (e.g., their ability to act as "conformational locks").[29] The authors determined that these interactions were relatively weak in comparison to the degree of delocalization along the backbone, and thus the energy of delocalization played a far greater role in determining the torsional profile.

These previous works highlight the difficulty in accurately modeling many sterically hindered conjugated polymers (e.g., poly(naphthalene diimide) (PNDI)-based polymers) and offer improvements upon the conventional TS method for doing so. Additionally, for sterically hindered polymers, the high steric clashes that occur near planarity can result in inaccurate calculations of the overall rigidity of the polymer, which is typically defined by the difference in energy between planarity (0° and 180°) and a break in planarity (90°).[30] Finally, the conventional nonbonded terms that handle high steric interactions are sensitive to minute changes in the placement of the atoms. As a result, the calculated energies become highly dependent on the input parameters for the model (e.g., initial configuration of the system, method of geometry optimization, choice of dihedral angle). Minute changes to the method parameters can yield substantially different calculations of nonbonded energies and thus overall torsional energies. Thus, the conventional TS method for applying nonbonded corrections to the torsional energy is not firmly connected to the molecular structure and therefore not universal.

To address the inaccuracy with which conventional approaches estimate the total torsional energy in conjugated polymers, we developed a method to determine the energy solely related to electronic delocalization. We term this method the "delocalization energy isolation method" (DE). To benchmark our method to the most accurate one reported in the literature, we chose the modified torsional scan method developed by DuBay et al.[21] and employed by Jackson et al. (which we simply refer to as the "torsional scan method"). This method has greater accuracy compared to a basic, more common torsional scan that does not correct for nonbonded interactions.[18] Quantum mechanical data are used in both the torsional scan method ("QM-TS") and the delocalization energy method ("QM-DE"). To verify that the estimates of the rigidity were accurate, the quantum mechanical data were incorporated into a force field for molecular dynamics

simulation based on the ubiquitous OPLS force field (commonly used to model organic liquids and materials).[31] The force field utilizing the torsional scan method is termed OPLS-TS,[18] and the force field optimized with the delocalization energy isolation method is termed OPLS-DE.

The DE method is described in Figure 1. First, a conventional torsional scan, based on the seminal work by
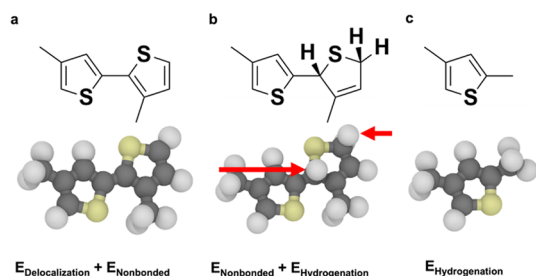

Figure 1. Overview of parametrization of the DE method. Initial torsional scans are performed (a) with a simple dimer (bi(3-methylthiophene)), rotating the dihedral angle through all possible configurations. The dimer is then (b) hydrogenated, with one of the hydrogen atoms bonded to the carbon atom involved in the dimer bond. The C−H bond is typically perpendicular to the plane of the ring. An additional hydrogen is also added on the end of the dimer, i.e., on the carbon which would continue the chain in a polymer. This provides an estimation of the nonbonded energy of the dimer, as any energy due to electron delocalization between dimers is blocked by the hydrogen. Additionally, a version of the dimer where (c) one of the monomers is entirely replaced by a methyl group is used. In this structure, one of the hydrogen atoms on the methyl group is in the same location as in the hydrogenated dimer to control for any added energy caused by the unphysical hydrogen atom.

Marcon and Raos,[18,32] is conducted by optimizing the geometry of the planar conformation of the dimer. Then, we calculate the potential energy curve as a function of increasing torsion angle between the monomers (Figure 1a). The energy calculated from the torsional scan has contributions from both electronic delocalization, $\Delta E_{Delocalization}$, and nonbonded interactions, $\Delta E_{Nonbonded}$, such that

$$\Delta E_{Dimer} = \Delta E_{Total} = \Delta E_{Delocalization} + \Delta E_{Nonbonded} \qquad (1)$$

We then separate $\Delta E_{Nonbonded}$ from $\Delta E_{Delocalization}$ to extract the energy due solely to delocalization. To approximate $\Delta E_{Nonbonded}$, an identical torsional scan is performed on a variation of the structure, where one monomer is dually hydrogenated (Figures 1b and S1a). The placement of a hydrogen atom in the π-system (specifically, at the point of attachment with the aromatic monomer) interrupts the delocalization of electrons. Thus, the calculated energy of the hydrogenated dimer is taken as being primarily due to nonbonded forces in the system, $\Delta E_{nonbonded}$, plus energy related to the unphysical placement of the hydrogen atom in the π-system, $\Delta E_{Hydrogenation}$, such that

$$\Delta E_{Hydrogenated\ Dimer} = \Delta E_{Nonbonded} + \Delta E_{Hydrogenation} \qquad (2)$$

The energetics from the placement of the second hydrogen atom should remain relatively constant for all torsional angles. Finally, to separate the energy of the hydrogen atom in the π-system from the nonbonded contributions, the molecule is modified such that the hydrogenated monomer is replaced by a methyl group (Figures 1c and S1b). In this methyl group, one of the hydrogen atoms is placed in the same perpendicular

position as in the hydrogenated dimer. The other two hydrogen atoms are oriented in the same directions as the carbon atoms attached to the (2, 5) positions of the unsaturated monomer. The position of the hydrogen atoms thus mimics the position of the atoms in the hydrogenated dimer. The methylated monomer provides an approximation of the energy of the placement of the unphysical hydrogen atom, $\Delta E_{Hydrogenation}$, such that

$$\Delta E_{Methylated\ Monomer} = \Delta E_{Hydrogenation} \qquad (3)$$

The energy (as calculated using a torsional scan) of this methylated monomer is subtracted from the energy of the hydrogenated dimer to estimate the total contribution of nonbonded energy, $\Delta E_{Nonbonded}$, where

$$\Delta E_{Nonbonded} = \Delta E_{Hydrogenated\ Dimer} - \Delta E_{Methylated\ Monomer} \qquad (4)$$

Finally, the nonbonded energy is subtracted from the energy of the pure dimer to obtain an estimation of the delocalization energy:

$$\Delta E_{Delocalization} = \Delta E_{dimer} - \Delta E_{Nonbonded} \qquad (5)$$

In doing so, both the energy of delocalization and nonbonded energy in the system are isolated (Figure S2). For polymers in which the backbone structure contains more than one aromatic moiety, there exists a choice for which monomer to perform these modifications on, as either is sufficient to interrupt delocalization. We elect to perform the hydrogenation and methylation on the larger monomer due to the lower energetic penalties, although we show how the same modifications on the smaller monomer affect the torsional energy (Figure S3). To summarize briefly, hydrogenating the smaller monomer produces a similar torsional profile as the larger monomer, but replacing the smaller monomer with a methyl group results in a larger penalty at high torsional angles. As such, this alternative method results in higher torsional barriers at high torsional angles, particularly around 180° (Figure S2).

We had three goals in attempting to account for these nonbonded interactions: accuracy, universality, and understandability. Of these goals, the most fundamental is accuracy because an accurate understanding of the rigidity of a conjugated polymer chain will allow for a better understanding of both electronic and mechanical properties. Indeed, previous work has shown that the rigidity of the semiconducting backbone is closely related to both the charge transport of a polymer chain[9,33] as well as the elastic modulus[34−36] in a solid film. The next goal was to build a universal model that could be used to characterize any conjugated polymer. While early studies with conjugated polymers tended to focus exclusively on poly(3-alkylthiophene) (P3AT) derivatives, the field is no longer dominated by a single polymer.[37] Instead, the emergence of donor−acceptor (D−A) polymers has resulted in the development of a diverse array of conjugated polymers applied to all areas of organic electronics.[38] For example, families of poly(diketopyrrolopyrrole) (PDPP), poly-(naphthalene diimide) (PNDI), indacenodithiophene (IDT), and poly(benzodithiophene) (PBDT) based backbone structures are all commonly used in organic transistors and solar cells.[39−42] Therefore, computational models must be able to accurately handle a wide (and growing) range of polymer structures and to allow for the comparison between polymers. An additional benefit of such universality is that advancements in computational modeling are also applicable to fused-ring

electron acceptors, which have dominated recent organic solar cell literature due to the high power conversion efficiencies of the devices they enable.[43] Finally, we aimed to develop a method that generates easily understandable data to guide both physical experiments and the rational design of conjugated polymers.

■ EXPERIMENTAL METHODS

Force Field Parametrization. QM calculations at the MP2 level of theory, performed using the Q-Chem package,[44] were used to measure the fundamental planarization energy of the conjugated polymer systems since MP2 has been shown to provide an excellent compromise between accuracy and computational cost.[18,19,25] Additionally, wave function based methods such as MP2 can provide insights into underlying physics behind nonbonded interactions not easily obtained by electronic structure density functional theory (DFT) calculations without specialized corrections.[45,46]

Our strategy for generating QM data for both the TS and DE methods (QM-DE and QM-TS) considers dimers—as opposed to oligomers—for several reasons. First, the literature is varied regarding how many monomers outside of the central dihedral torsion, if any, are necessary to accurately reflect the energy.[7,28,32,47,48] Additionally, these monomers are typically kept consistently coplanar with the monomers undergoing torsion in computational models, whereas in reality torsion between all monomers will constantly shift as the conformation of the polymer evolves. As such, we focus entirely on the energetics associated with the local breaks in conjugation between adjacent monomers. Electronic delocalization between adjacent monomers is the largest source of delocalization energy here and thus is the focus.

MP2 calculations with the resolution of identity (RI-MP2) using the cc-pvtz basis set were performed on three systems: (1) the fully conjugated dimers, (2) the hydrogenated dimers, and (3) dimers in which one of the monomers was replaced by a methyl group entirely (with the hydrogen atoms oriented similarly to the hydrogenated dimer). In all systems, the side chains were replaced with methyl groups to reduce computational time while maintaining electronic delocalization between the π-systems. For the hydrogenated dimer, two hydrogen atoms were added to the carbons at the (2, 5) positions. For the carbon atom not bonded to the opposing monomer, the hydrogen atom was placed in a conventional configuration. For the centrally bonded carbon atom in the dimer, the hydrogen atom was placed orthogonal to the plane of the ring to block any π-orbital delocalization. For the methylated dimer, the hydrogen atoms in the methyl group were manipulated to replicate the placement of atoms in the dimer. Two of the hydrogen atoms were attached in the directions of the bonded carbon atoms in the dimer, scaled to be at equilibrium distance (1.08 Å). The third hydrogen was placed in the same location as the nonphysical hydrogen (as is in the hydrogenated dimer). The increased energy from the hydrogen not being placed in an equilibrium position was thus compensated by subtracting the energy of the methylated dimer from the energy of the hydrogenated dimer. A methyl group was used instead of the full monomer to minimize nonbonded interactions with the remaining monomer while maintaining the energy related to the placement of the nonphysical hydrogen. The remaining energies were fit by an OPLS-style dihedral model, where the fitting was performed using a Levenberg−Marquardt algorithm. For the OPLS-TS model, the torsional scan energy was slightly modified to define the energy of backbone torsion in a conjugated polymer. Prior to the torsional scan, geometries of the dimers were optimized at the B3LYP level of theory with a 6-31+G** basis set in order to minimize steric interactions.[18] During the torsional scan, the structures were held rigid while the dihedral angle was varied. To correct for nonbonded effects within the system, the energy calculated from the nonbonded component (i.e., van der Waals and electrostatic interactions) of the OPLS basis set was subtracted from the overall energy given by the torsional scan. To calculate the torsional energy between conjugated rings in the modified OPLS-DE force field, the isolated delocalization energy was used instead of the total calculated energy from the torsional scan.

Verification of Force Field Accuracy. We obtained diverse structures of the gas-phase dimer for each conjugated polymer system by means of constant temperature (298 K)−constant volume (i.e., NVT) MD simulations with LAMMPS.[49] These structures were obtained by allowing aromatic rings in the conjugated backbone to rotate while holding their internal structures as rigid bodies. In other words, the aromatic rings could rotate but not bend. The conformation of the dimer was recorded every 100 ps, and the resulting structures used as input to a RI-MP2 QM calculation. The relative QM energies of each configuration was then compared to that obtained from our force field based simulations employing either the OPLS-TS or the OPLS-DE method. This comparison approximated how effective the OPLS-DE characterization was compared to OPLS-TS for modeling interactions between monomers. The energy difference between each dimer state was used (rather than comparison to a reference state) to normalize any potential idiosyncrasies of a reference state (e.g., incorrect calculation of the energy at planarity).

Bulk-Phase Simulations and Characterization. Simulations of each conjugated polymer were performed for 30 polymer chains, with each chain containing 30 monomers. The initial torsional angles between monomer rings were determined randomly using Boltzmann-weighted probabilities of each torsional angle. Simulations were performed between a model determined using the (1) OPLS-TS and (2) OPLS-DE force fields. These simulations provided a comparison of the torsional characterization of each model on the morphology of the bulk phase. To determine the weighted probabilities, these polymer chains were placed in a simulation box by PackMol and run for 20 ps in the microcanonical (constant particles N, volume V, and energy E or NVE) ensemble.[50] The equilibrium density of each system was then obtained by simulation in the constant pressure (1 bar)−constant temperature (NPT) ensemble, where the system was allowed to equilibrate for 5 ns at 400 K, before being cooled to 300 K over 0.5 ns. Each system was then simulated in the NVT ensemble, heating from 400 to 800 K over 2 ns, held at 800 K for 5 ns, and then cooled to 300 K over 2 ns for proper equilibration. Finally, the long-term production dynamics were run for 10 ns in the NPT ensemble, with snapshots (atomic positions) of the corresponding bulk-phase morphology taken every nanosecond. For all NVT and NPT simulations, a Nosé−Hoover thermostat with a damping parameter of 100 fs was used. For all NPT simulations, a Nosé−Hoover barostat with a damping parameter of 1 ps was used.
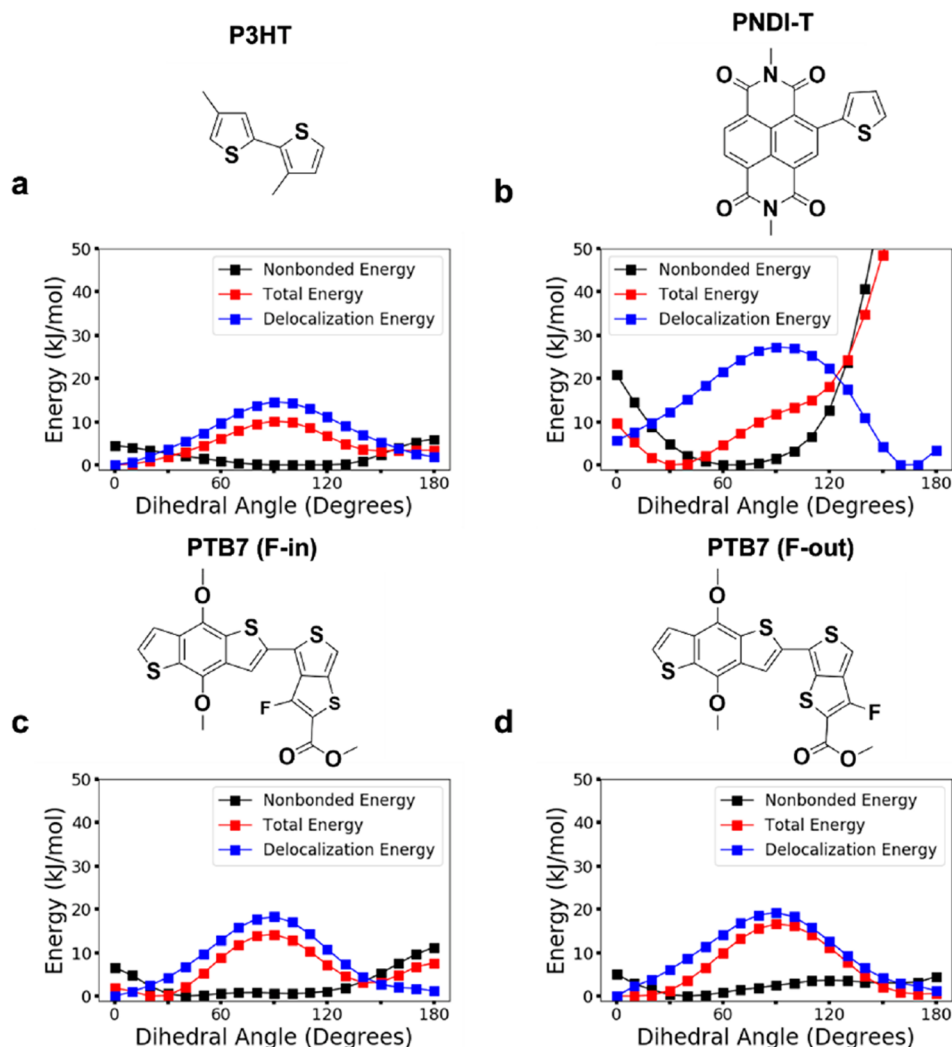
Figure 2. Estimations of the types of energy as used in the DE method, showing the pure delocalization energy (blue), nonbonded interactions (black), and total energy of the TS method (red). Notably, the minimum energy for all three types of energy is set to zero, so the energies are not purely additive. In all three polymers, nonbonded interactions (namely, steric hindrance) serve to destabilize the planar conformation. The energies are shown for (a) P3HT, (b) PNDI-T, and (c) PTB7 with the fluorine on the interior ("F-in") and (d) PTB7 with the fluorine on the exterior ("F-out"). All side chains for these polymers were replaced with methyl groups for calculations of energy as shown above.

RESULTS AND DISCUSSION

QM Calculated Nonbonded and Delocalization Energies. We used the DE method to estimate the nonbonded and delocalization energies of three polymers—poly(3-hexylthiophene) (P3HT), polythieno[3,4-*b*]-thiophene-*co*-benzodithiophene (PTB7), and poly(naphthalene diimide) with a single bridging thiophene (PNDI-T)—as shown in Figure 2. The delocalization energy determined by the DE method was then compared to the total energy in the DE method. We found that the isolated delocalization energy differs significantly from the total energy obtained from the TS method. For all three polymers, the nonbonded energy increased most significantly when the monomers were coplanar with one another. There were two major consequences of this result. First, the nonbonded energy calculated by the TS method rose sharply near planarity, even with a QM geometry optimization. The rise in energy was particularly high for PNDI-T (due to the steric clash between the oxygen and the sulfur, Figure S4) and resulted in torsional energies which deviate significantly from any attempted fit to an OPLS-style

torsion. Second, the high correction for the nonbonded energy could result in a highly different calculation of the difference between planarity and antiplanarity (90°). This skew means that a fundamental metric of torsion in π-conjugated polymers was difficult or impossible to determine from the TS method.

As a specific illustrative case, consider PTB7, which has two regioisomeric monomer types: one with the fluorine atom pointed away from the benzodithiophene (F-out) and the other with the fluorine atom pointed toward the benzodithiophene (F-in). During the synthesis, the orientation of the fluorine-substituted thieno[3,4-*b*]thiophene is statistical (essentially random). The two regioisomers have similar electronic structures, however, and thus the planarization energy of the two regioisomers predicted from electronic delocalization alone should also be similar. Nevertheless, the TS method calculated diverging energies for the two different configurations (Figures 2c and 2d). Previous studies of PTB7 have resulted in such different characterizations of torsional energy that the two conformations were treated entirely differently, despite their nearly isoelectronic structure.[18]
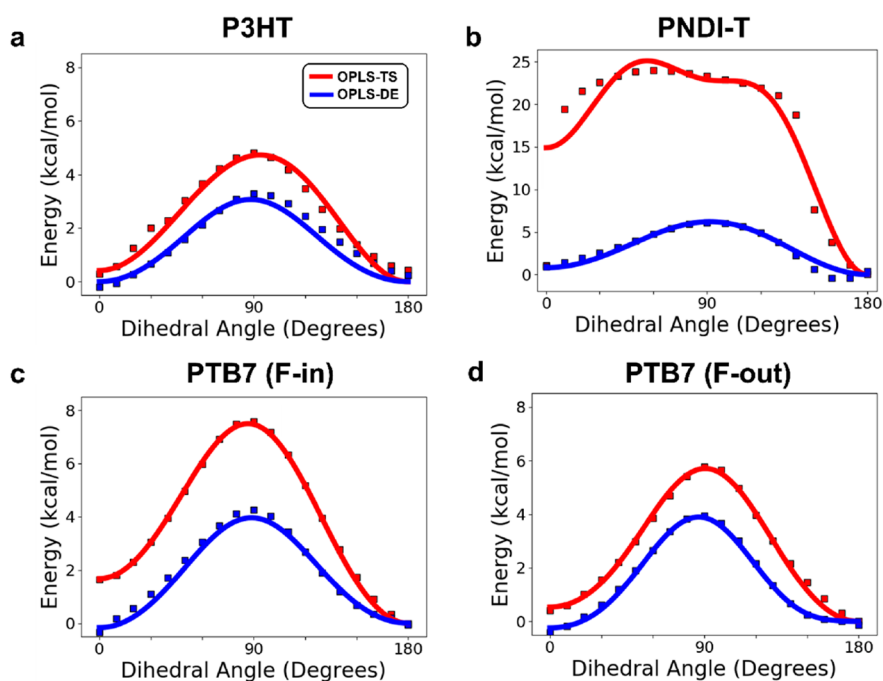
Figure 3. Difference in energy between the OPLS-DE and OPLS-TS methods for (a) P3HT, (b) PNDI-T, (c) the F-in conformation of PTB7, and (d) the F-out conformation of PTB7.
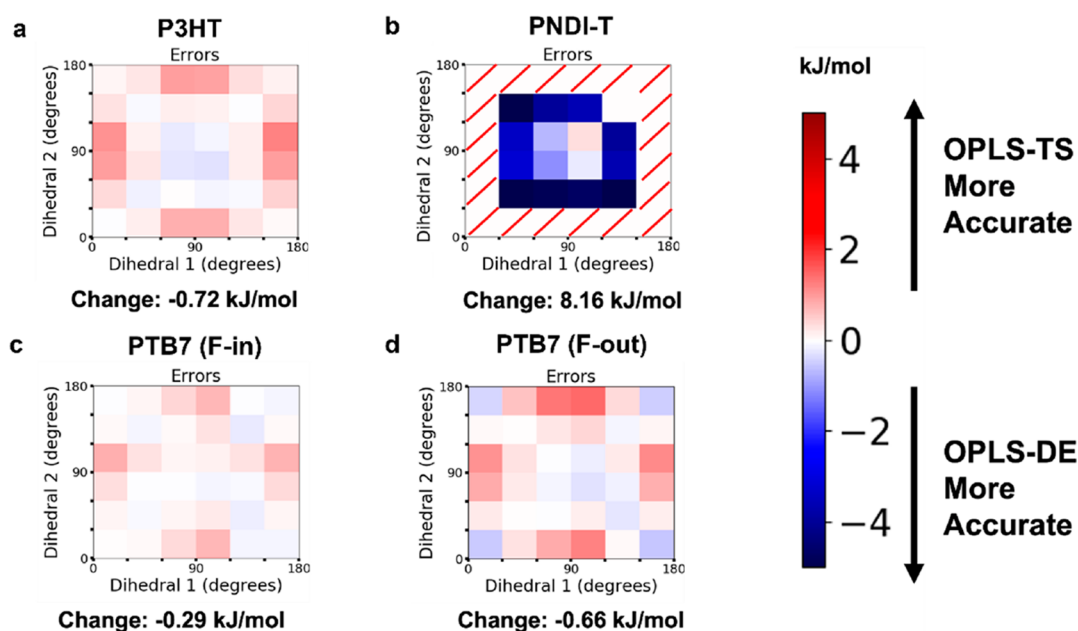
Figure 4. Comparison of the calculated energy of torsion for (a) P3HT, (b) PNDI-T, (c) the F-in configuration of PTB7, and (d) the F-out configuration of PTB7 using the OPLS-TS and OPLS-DE methods. The relative accuracy of each method is determined by comparison to energies derived from quantum mechanical calculations. Red indicates that the OPLS-TS force field performs better, while blue indicates the OPLS-DE force field performs better. A red slash through a box indicates that no configurations of dimers with those dihedral angles were sampled.

The different energies given by the TS method therefore do not precisely estimate a rigidifying energy of PTB7, for which the underlying fundamental rigidifying energetics are obscured by steric forces. When the F-out dimer was considered, the presence of the sulfur results in a smoother surface; there is no hydrogen atom protruding from a carbon to generate an unfavorable steric interaction (e.g., steric clash) with the benzodithiophene unit. Thus, the PTB7 F-out coupling motif

resulted in the lowest nonbonded energies of all three polymer systems considered. There was a slight increase in total energy in the TS method at planarity, and the energies of delocalization and total energy were approximately equal. In contrast, when considering the F-in dimer, the torsional scan was significantly affected by the nonbonded energies. For example, when the fluorine substituent and the sulfur atom of the benzodithiophene were on opposite sides, the difference in
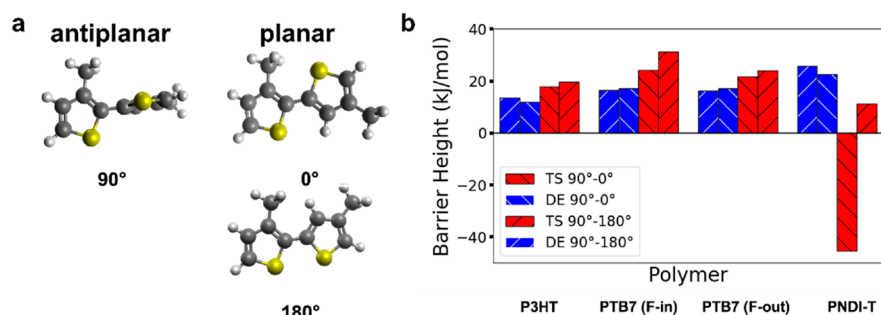
Figure 5. (a) The planarization energy was estimated from the difference in energy of (1) dimers with 90° and 0° of torsion ("90°−0°") and (2) dimers with 90° and 180° of torsion ("90°−180°"). (b) Relative planarization energies of P3HT, PTB7 (F-in and F-out), and PNDI-T as determined using the DE and TS methods.

energy between a 0° and 90° dihedral angle was approximately 16 kJ/mol. When the fluorine substituent of the thieno[3,4-b]thiophene unit and the sulfur atom in the benzodithiophene ring were adjacent, the difference in energy between 0° and 90° of torsion was only approximately 7.5 kJ/mol. Given that this energy determined by the torsional scan is the only force in a simulation that will push the polymers toward planarity—and that nonbonded forces are already separately accounted for (e.g., through Coulomb and Lennard-Jones potentials)—the TS method will result in a highly twisted polymer model. We note that this effect was observed irrespective of the fact that every "F-in" coupling results in an "F-out" coupling with the benzodithiophene of the adjacent monomer (Figure 2d). Nevertheless, 50% of the dihedral interactions were of the "F-in" monomer type and will thus contribute to twisted structures with highly reduced planarizing forces.

We then fit both the quantum mechanical energies from the torsional scan (QM-TS) and quantum mechanical energies of the estimated pure delocalization energy (QM-DE) (Figure 3). A dihedral style used by a conventional OPLS force field was used to facilitate application in MD or Monte Carlo simulations. Then, the QM and force field energies were compared as a function of torsional angle to determine how well the methods allow for simple approximation of quantum mechanical energy (Figure 3). For P3HT, PNDI-T, and the F-in conformation of PTB7, complete breaking of planarity (i.e., a 90° torsional angle) was less penalized in terms of calculated energy when using the OPLS-DE method. After fitting both the QM-TS and QM-DE data to an OPLS-style dihedral model, differences between the two models were similar to those observed in the unfit (Figure 2) delocalization energies. The largest differences were seen in PNDI-T, where the OPLS-TS method resulted in a highly inaccurate fit. Finally, we compared the accuracy of the PNDI-T torsional scan method to the simple raw torsional scan of PNDI-T, as the correction of the nonbonded energy results in highly skewed energy (Figure S5). We found that the energies of the dimer obtained from the TS method were different at planarity (i.e., at 0° and 180°), making the fundamental rigidity of the polymers difficult to estimate and compare without further MD simulations. The difference between the energy of planar dimers was particularly high when steric hindrance was high, such as for PNDI-T and the F-in structure of PTB7.

To compare the relative accuracy of the DE and TS methods for determining the fundamental planarization energy of conjugated polymers, the torsional energies of each polymer were used as parameters in an OPLS force field. Dimers were

then allowed to rotate freely in a vacuum at high temperature (i.e., with no torsional barrier). The resulting torsional force field energies (as derived from the OPLS-DE and OPLS-TS methods) were compared to quantum mechanical calculations at the RI-MP2 level. The relative accuracy of the calculated difference in energy (with respect to the dihedral angle) for randomized configurations of each dimer is shown in Figure 4. As expected, the DE method slightly underestimated the overall torsional energy of each polymer. This underestimation was due to the estimation of the nonbonded forces with an analogue dimer (i.e., a hydrogenated form of the dimer). However, the relative accuracy of the OPLS-DE and OPLS-TS methods were highly similar for PTB7 and P3HT (within 1 kJ/mol). Likewise, the OPLS-DE method showed a greater improvement in accuracy when calculating the energy of the F-out variation (as opposed to the F-in counterpart) due to the difference in steric hindrance between the monomer variations. We observe that the DE method is least accurate when comparing 90° of torsion and 0° of torsion, as nonbonded effects are not accounted for. However, what is most striking is the significant increase in accuracy when calculating the torsional energy of the highly sterically hindered PNDI-T (8.16 kJ/mol) with the OPLS-DE method. Additional simulations comparing the OPLS-DE method to a more basic torsional scan method (i.e., one in which no corrections are made for nonbonded interactions) showed that the relative accuracy of PNDI-T was actually worsened by the consideration of nonbonded OPLS corrections in our OPLS-TS method (Figure S3). This decrease in accuracy was attributed to the classical molecular mechanics potential (as implemented in the OPLS force field) used to correct for nonbonded forces, which resulted in exponential increases in the calculated energy for sterically hindered configurations of PNDI-T.

We note that in our high-temperature simulations steric hindrance prevented PNDI-T from exploring configurations in which both dihedrals were near planarity or antiplanarity. These simulations suggest that such configurations are highly unfavorable due to steric clashes under equilibrium. However, these configurations are far more likely to occur when considering nonequilibrium processes (e.g., stretching, or similar mechanical deformation of the solid film). In such cases, we expect the energy of these states to be substantially more accurate when calculated by OPLS-DE due to the overestimation of nonbonded energy correction from conventional OPLS-TS methods. Thus, these findings suggest that the DE method is both (1) accurate for calculating the fundamental torsional energy for any given polymer and (2)
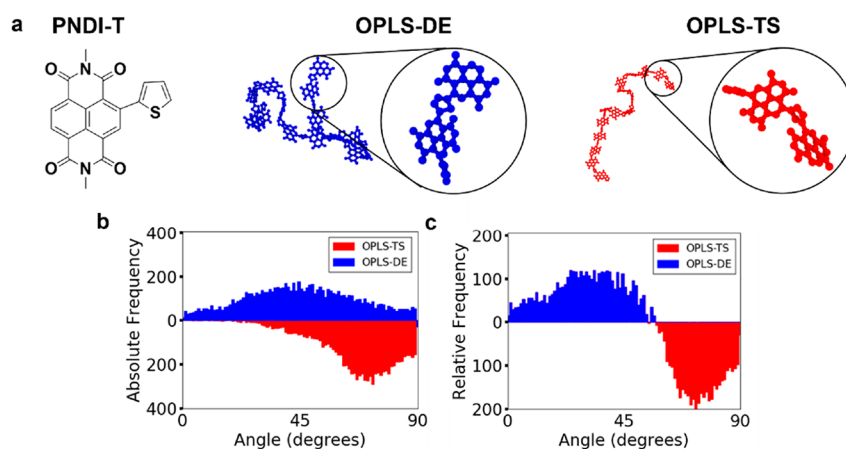
Figure 6. (a) Visualization of the morphology of a single PDNI-T chain as modeled using an OPLS-DE (blue) or OPLS-TS (red) force field. Side chains were removed to make torsional angles clearly visible. A zoomed-in image of the first four monomers (as characterized in the simulation) is provided. (b) Total distribution and (c) net difference of dihedral angles extracted from the molecular dynamics (MD) simulations of PNDI-T. Angles were calculated by deviation from planarity such that 0° and 180° were considered identical (thus the calculated frequencies for 90°−180° are not shown).

able to model highly sterically hindered polymers (that are unsuitable for the TS method).

The torsional barrier to rotation (i.e., energy of planarization) was calculated for each polymer using both the DE and TS methods (Figure 5). We calculated the torsional barrier by comparing the calculated energy of each polymer at antiplanarity (90° dihedral angle) and planarity (0° or 180°) using both DE and TS methods (Figure 5a). The 0° dimer calculations are termed "90°−0°", while the 180° dimer calculations are labeled "90°−180°". In planar (0° and 180°) conformations, the energy associated with delocalization should be comparable because electrons should be able to delocalize as easily in one conformation as the other. Therefore, we expect similar energetic minima at these torsional angles. Additionally, we expect the energetic maxima to be located at perfect antiplanarity (90°). Thus, both calculations of planarization energy should be comparable if the model accurately represents the fundamental delocalization forces that rigidify a polymer.

The DE method outperformed the TS method for all polymers in terms of relative precision, giving highly similar energies (only varying by a maximum of 3 kJ/mol) for both calculation styles when applied to each polymer (Figure 5b). This precision indicates that the maximum calculated value of the torsional barrier was always at or close to perfect planarity, while the minimum value was always at or close to perfect antiplanarity. Both calculated torsional barriers were within 1.5 kJ/mol of one another for P3HT and PTB7 (F-in and F-out) when OPLS-DE was used. The calculations for PTB7 were highly precise not only between the 90°−0° and 90°−180° methods but also between the two monomer variants. All four calculations of the torsional barrier for PTB7 were within 1.5 kJ/mol. PNDI-T had a slightly larger mismatch between the 90°−0° and 90°−180° calculations (3 kJ/mol) due to the massive steric forces within these conformations, resulting in some noise within the calculation of the delocalization energy.

In contrast, the precision of the TS method varied significantly in calculating the torsional barrier. The calculations for P3HT were relatively precise due to the moderate amount of steric hindrance, resulting in a difference of 2 kJ/mol. The same was true for the F-out variation of PTB7 (3 kJ/

mol difference). However, the F-in variation of PTB7 showed torsional barriers that differed by up to 10 kJ/mol between the two methods of calculation. Finally, the OPLS-TS method gave a highly inaccurate fit for PNDI-T, with calculations that differed by 50 kJ/mol. The energy for PNDI-T at 0° was significantly higher than in the antiplanar configuration, resulting in a negative torsional barrier for the 90°−0° calculation. In comparison, the calculated energy at 180° was far lower, despite the fact that the two planar configurations are expected to have the same delocalization energy. The 90°−180° calculation of the planarization energy was relatively small, even comparable to that of P3HT, despite the fact that PNDI-T is a donor−acceptor polymer with (1) significant differences in the electronegativity between the monomers (i.e., a more rigid backbone due to the push−pull effect) and (2) far greater steric hindrance.

We end our analysis of Figure 5 by considering how the calculated torsional barriers could be interpreted for experimental design. While OPLS-TS performed well for P3HT, both the precision and accuracy of the calculated torsional barrier suffered for PTB7 and PNDI-T. In comparison, the DE method is more precise in its determination (and interpretation) of the planarization energy of each polymer: P3HT (~13 kJ/mol of planarization energy) < PTB7 (~17 kJ/mol for both the F-in and F-out structures) < PNDI-T (~25 kJ/mol). The planarization energy of these polymers correlates with (1) the increasing disparity in electronegativity along the backbone and (2) the increasing size of the π-system (from P3HT to PTB7 to PNDI-T). These findings are consistent with experimental expectations, in particular due to the similarity of both PTB7 dimers and intuition regarding D−A polymer backbone rigidity.[51] As such, the DE method provides a facile method for observing and comparing the primary driving force of planarization in conjugated backbones (i.e., electronic delocalization) without further MD simulations typically used to determine backbone rigidity.

Large-Scale Polymer Morphology. Thus far, our findings have suggested that the DE method is both more accurate and more precise for modeling highly sterically hindered polymers. To predict how the morphology of PNDI-

T is dependent on an OPLS-TS or OPLS-DE force field, molecular dynamics simulations were performed (Figure 6a). We found that the morphology of PNDI-T was significantly more planar (as calculated by inter-ring torsion) when modeled using the OPLS-DE force field (Figure 6b).

PDNI-T showed a clear difference between of the accuracy of the two force fields based on the TS and DE methods. Without proper correction of the nonbonded energies, the OPLS-TS force field yielded a maximum frequency of torsional angles at ~70°. In this model, all torsional angles above 45° had large frequencies while all angles below 45° had very low frequencies. In contrast, the OPLS-DE distribution resembles a normal distribution centered around 40°. The OPLS-DE model fits well with our current understanding of NDI polymers: while these polymers are often termed highly twisted, they do not present configurations that are nearly entirely antiplanar, as is suggested in the OPLS-TS model. Theoretical models[52] posit an energetic minimum around 40°, consistent with the OPLS-DE results. Notably, torsional angles commonly above 45° would present a serious obstacle to π-stacking, which occurs to a significant degree in NDI polymers.[53] Thus, these findings suggest that the OPLS-DE model is a better predictor of the morphology of highly sterically hindered conjugated polymers in comparison to its OPLS-TS counterpart.

CONCLUSIONS

In this work, we devise a method for isolating the energy of delocalization for any arbitrary conjugated polymer from the nonbonded energy. When directly inserted as a torsional potential into a standard OPLS force field, the delocalization energy ("DE") method showed accuracies within 1 kJ/mol for two polymers (PTB7 and P3HT) that are handled well by the torsional scan ("TS") method. However, the DE method significantly increased the accuracy of the calculations of torsional energy for a highly sterically hindered polymer (PNDI-T, 8.16 kJ/mol) relative to the TS method (when compared to quantum mechanical calculations). Likewise, the DE method greatly increased the precision of the calculated torsional barrier for each of the three polymers. As a result, the predicted morphology of PNDI-T differed significantly when modeled using an OPLS-DE force field as opposed to an OPLS-TS force field. With a correction for the nonbonded energies, the PNDI-T polymer chain was significantly more planar as measured by inter-ring torsion, which validates other theoretical models and experimental findings. Thus, the DE method improves upon the TS method in accuracy, universality, and understandability for the modeling of conjugated polymers.

Donor–acceptor polymers have become increasingly complex in structure, resulting in polymers with greater steric hindrance that cannot be accurately modeled using the TS method. The DE method presents a path forward for universal modeling of highly sterically hindered polymers by decoupling fundamental energies associated with electronic delocalization and nonbonded forces. Although increases to the accuracy of PNDI-T are relatively small at low dihedral angles, it is worth noting that the relative accuracy of the DE method occurred with no attempt at accounting for potential nonbonded forces. Further corrections to the force field potential through methods such as machine learning could make the method substantially more accurate than the TS method. Additionally, high dihedral twists are more likely to occur for non-

equilibrium processes (e.g., stretching, bending, and other modes of deformation). Therefore, simulations of such, where highly sterically hindered conformations are more likely to occur, could potentially see much larger improvements in accuracy using the DE method. Thus, the DE method could be broadly applied to other models by using a similar series of calculations to decouple energies. We also note that simulations in this study were conducted only on dimers rather than oligomers. However, a deeper understanding of how distant monomers affect the rigidifying forces within the backbone may further improve the accuracy of the model and facilitate the simulation of conjugated polymers at larger domain scales (e.g., longer polymer chains, bulk morphology within a thin film). Likewise, future work could possibly benefit from examining relationships between experimental characterizations of semiconducting polymers and the decoupled energies calculated using the DE method. Finally, the DE method should be effective for a number of other materials common to organic electronics (e.g., conjugated organic ligands in metal−organic frameworks, small molecule acceptors in organic electronics, liquid crystal mesogens) for both understanding fundamental forces and guiding experimental design as well as other sterically hindered conjugated polymers.

■ ASSOCIATED CONTENT

Supporting Information

The Supporting Information is available free of charge at https://pubs.acs.org/doi/10.1021/acs.jpcb.2c08843.

Figures S1−S5 (chemical structures used, example torsional scans, comparison of structural modifications on the larger and smaller monomers for PDNI-T and PTB7, visualization of PNDI-T steric clash, calculated energy of torsion for PNDI-T with no nonbonded corrections) (PDF)

LAMMPS input files (ZIP)

■ AUTHOR INFORMATION

Corresponding Authors

Tod A. Pascal − *Department of NanoEngineering, University of California, San Diego, La Jolla, California 92093-0448, United States;* orcid.org/0000-0003-2096-1143; Email: tpascal@eng.ucsd.edu

Darren J. Lipomi − *Department of NanoEngineering, University of California, San Diego, La Jolla, California 92093-0448, United States;* orcid.org/0000-0002-5808-7765; Email: dlipomi@eng.ucsd.edu

Authors

Andrew T. Kleinschmidt − *Department of NanoEngineering, University of California, San Diego, La Jolla, California 92093-0448, United States;* orcid.org/0000-0002-6036-6878

Alexander X. Chen − *Department of NanoEngineering, University of California, San Diego, La Jolla, California 92093-0448, United States;* orcid.org/0000-0003-1919-6755

Robert S. Ramji − *Department of NanoEngineering, University of California, San Diego, La Jolla, California 92093-0448, United States*

Complete contact information is available at:
https://pubs.acs.org/10.1021/acs.jpcb.2c08843

REFERENCES

(1) Lim, K. C.; Kapitulnik, A.; Zacher, R.; Casalnuovo, S.; Wudl, F.; Heeger, A. J. Polydiacetylene Macromolecules in Solution: Rods, Coils and Gels. *Polydiacetylenes* **1985**, 257−290.

(2) Beaujuge, P. M.; Amb, C. M.; Reynolds, J. R. Spectral Engineering in π-Conjugated Polymers with Intramolecular Donor-Acceptor Interactions. *Acc. Chem. Res.* **2010**, *43*, 1396−1407.

(3) Fratini, S.; Nikolka, M.; Salleo, A.; Schweicher, G.; Sirringhaus, H. Charge Transport in High-Mobility Conjugated Polymers and Molecular Semiconductors. *Nat. Mater.* **2020**, *19*, 491−502.

(4) Yu, Z. Di; Lu, Y.; Wang, J. Y.; Pei, J. Conformation Control of Conjugated Polymers. *Chem. - A Eur. J.* **2020**, *26*, 16194−16205.

(5) Tamai, Y. Delocalization Boosts Charge Separation in Organic Solar Cells. *Polym. J. 2020 527* **2020**, *52*, 691−700.

(6) Noriega, R.; Rivnay, J.; Vandewal, K.; Koch, F. P. V.; Stingelin, N.; Smith, P.; Toney, M. F.; Salleo, A. A General Relationship between Disorder, Aggregation and Charge Transport in Conjugated Polymers. *Nat. Mater.* **2013**, *12*, 1038−1044.

(7) Lin, J. B.; Jin, Y.; Lopez, S. A.; Druckerman, N.; Wheeler, S. E.; Houk, K. N. Torsional Barriers to Rotation and Planarization in Heterocyclic Oligomers of Value in Organic Electronics. *J. Chem. Theory Comput.* **2017**, *13*, 5624−5638.

(8) Hwang, H.; Kim, Y.; Kang, M.; Lee, M. H.; Heo, Y. J.; Kim, D. Y. A Conjugated Polymer with High Planarity and Extended π-Electron Delocalization: Via a Quinoid Structure Prepared by Short Synthetic Steps. *Polym. Chem.* **2017**, *8*, 361−365.

(9) Cao, Z.; Leng, M.; Cao, Y.; Gu, X.; Fang, L. How Rigid Are Conjugated Non-Ladder and Ladder Polymers? *J. Polym. Sci.* **2022**, *60*, 298−310.

(10) Tsumura, A.; Koezuka, H.; Ando, T. Macromolecular Electronic Device: Field-effect Transistor with a Polythiophene Thin Film. *Appl. Phys. Lett.* **1986**, *49*, 1210.

(11) Chamberlain, G. A. Organic Solar Cells: A Review. *Sol. Cells* **1983**, *8*, 47−83.

(12) Crone, B.; Dodabalapur, A.; Gelperin, A.; Torsi, L.; Katz, H. E.; Lovinger, A. J.; Bao, B. Electronic Sensing of Vapors with Organic Transistors. *Appl. Phys. Lett.* **2001**, *78*, 2229.

(13) Havinga, E. E.; ten Hoeve, W.; Wynberg, H. Alternate Donor-Acceptor Small-Band-Gap Semiconducting Polymers; Polysquaraines and Polycroconaines. *Synth. Met.* **1993**, *55*, 299−306.

(14) Beaujuge, P. M.; Fréchet, J. M. J. Molecular Design and Ordering Effects in π-Functional Materials for Transistor and Solar Cell Applications. *J. Am. Chem. Soc.* **2011**, *133*, 20009−20029.

(15) Zhang, X.; Bronstein, H.; Kronemeijer, A. J.; Smith, J.; Kim, Y.; Kline, R. J.; Richter, L. J.; Anthopoulos, T. D.; Sirringhaus, H.; et al. Molecular Origin of High Field-Effect Mobility in an Indacenodithiophene-Benzothiadiazole Copolymer. *Nat. Comun.* **2013**, *4*, 1−9.

(16) Northrup, J. E. Mobility Enhancement in Polymer Organic Semiconductors Arising from Increased Interconnectivity at the Level of Polymer Segments. *Appl. Phys. Lett.* **2015**, *106*, 023303.

(17) Marcon, V.; Raos, G. Free Energies of Molecular Crystal Surfaces by Computer Simulation: Application to Tetrathiophene. *J. Am. Chem. Soc.* **2006**, *128*, 1408−1409.

(18) Jackson, N. E.; Kohlstedt, K. L.; Savoie, B. M.; Olvera de la Cruz, M.; Schatz, G. C.; Chen, L. X.; Ratner, M. A. Conformational Order in Aggregates of Conjugated Polymers. *J. Am. Chem. Soc.* **2015**, *137*, 6254−6262.

(19) Raos, G.; Famulari, A.; Marcon, V. Computational Reinvestigation of the Bithiophene Torsion Potential. *Chem. Phys. Lett.* **2003**, *379*, 364−372.

(20) Jackson, N. E.; Savoie, B. M.; Kohlstedt, K. L.; Olvera de la Cruz, M.; Schatz, G. C.; Chen, L. X.; Ratner, M. A. Controlling Conformations of Conjugated Polymers and Small Molecules: The Role of Nonbonding Interactions. *J. Am. Chem. Soc.* **2013**, *135*, 10475−10483.

(21) DuBay, K. H.; Hall, M. L.; Hughes, T. F.; Wu, C.; Reichman, D. R.; Friesner, R. A. Accurate Force Field Development for Modeling Conjugated Polymers. *J. Chem. Theory Comput.* **2012**, *8*, 4556−4569.

(22) Do, H.; Troisi, A. Developing Accurate Molecular Mechanics Force Fields for Conjugated Molecular Systems. *Phys. Chem. Chem. Phys.* **2015**, *17*, 25123−25132.

(23) Henry, M. M.; Jones, M. L.; Oosterhout, S. D.; Braunecker, W. A.; Kemper, T. W.; Larsen, R. E.; Kopidakis, N.; Toney, M. F.; Olson, D. C.; Jankowski, E. Simplified Models for Accelerated Structural Prediction of Conjugated Semiconducting Polymers. *J. Phys. Chem. C* **2017**, *121*, 26528−26538.

(24) Wildman, J.; Repiščák, P.; Paterson, M. J.; Galbraith, I. General Force-Field Parametrization Scheme for Molecular Dynamics Simulations of Conjugated Materials in Solution. *J. Chem. Theory Comput.* **2016**, *12*, 3813−3824.

(25) Wolf, C. M.; Guio, L.; Scheiwiller, S.; Pakhnyuk, V.; Luscombe, C.; Pozzo, L. D. Strategies for the Development of Conjugated Polymer Molecular Dynamics Force Fields Validated with Neutron and X-Ray Scattering. *ACS Polym. Au* **2021**, *1*, 134−152.

(26) Darling, S. B.; Sternberg, M. Importance of Side Chains and Backbone Length in Defect Modeling of Poly(3-Alkylthiophenes). *J. Phys. Chem. B* **2009**, *113*, 6215−6218.

(27) Thorley, K. J.; McCulloch, I. Why Are S-F and S-O Non-Covalent Interactions Stabilising? *J. Mater. Chem. C* **2018**, *6*, 12413−12421.

(28) Che, Y.; Perepichka, D. F. Quantifying Planarity in the Design of Organic Electronic Materials. *Angew. Chemie - Int. Ed.* **2021**, *60*, 1364−1373.

(29) Karunasena, C.; Li, S.; Heifner, M. C.; Ryno, S. M.; Risko, C. Reconsidering the Roles of Noncovalent Intramolecular "Locks" in Conjugated Molecules. *Chem. Mater.* **2021**, *33*, 9139−9151.

(30) Zhang, W.; Gomez, E. D.; Milner, S. T. Predicting Chain Dimensions of Semiflexible Polymers from Dihedral Potentials. *Macromolecules* **2014**, *47*, 6453−6461.

(31) Jorgensen, W. L.; Maxwell, D. S.; Tirado-Rives, J. Development and Testing of the OPLS All-Atom Force Field on Conformational Energetics and Properties of Organic Liquids. *J. Am. Chem. Soc.* **1996**, *118*, 11225−11236.

(32) Marcon, V.; Raos, G. Molecular Modeling of Crystalline Oligothiophenes: Testing and Development of Improved Force Fields. *J. Phys. Chem. B* **2004**, *108*, 18053−18064.

(33) Xu, Y.; Sun, H.; Li, W.; Lin, Y.-F.; Balestra, F.; Ghibaudo, G.; Noh, Y.-Y. Exploring the Charge Transport in Conjugated Polymers. *Adv. Mater.* **2017**, *29*, 1702729.

(34) Roth, B.; Savagatrup, S.; De Los Santos, N. V.; Hagemann, O.; Carlé, J. E.; Helgesen, M.; Livi, F.; Bundgaard, E.; Søndergaard, R. R.; et al. Mechanical Properties of a Library of Low-Band-Gap Polymers. *Chem. Mater.* **2016**, *28*, 2363−2373.

(35) Galuska, L.; McNutt, W.; Qian, Z.; Zhang, S.; Weller, D.; Dhakal, S.; King, E.; Morgan, S.; Azoulay, J.; et al. Impact of Backbone Rigidity on the Thermomechanical Properties of Semiconducting Polymers with Conjugation Break Spacers. *Macromolecules* **2020**, *53*, 6032−6042.

(36) Ding, Z.; Liu, D.; Zhao, K.; Han, Y. Optimizing Morphology to Trade Off Charge Transport and Mechanical Properties of Stretchable Conjugated Polymer Films. *Macromolecules* **2021**, *54*, 3907−3926.

(37) Kleinschmidt, A. T.; Root, S. E.; Lipomi, D. J. Poly(3-Hexylthiophene) (P3HT): Fruit Fly or Outlier in Organic Solar Cell Research? *J. Mater. Chem. A* **2017**, *5*, 11396−11400.

(38) Kim, M.; Ryu, S. U.; Park, S. A.; Choi, K.; Kim, T.; Chung, D.; Park, T.; et al. Donor-Acceptor-Conjugated Polymer for High-Performance Organic Field-Effect Transistors: A Progress Report. *Adv. Funct. Mater.* **2020**, *30*, 1904545.

(39) Bao, W. W.; Li, R.; Dai, Z. C.; Tang, J.; Shi, X.; Geng, J. T.; Deng, Z. F.; Hua, J. Diketopyrrolopyrrole (DPP)-Based Materials and Its Applications: A Review. *Front. Chem.* **2020**, *8*, 679.

(40) Zhou, N.; Facchetti, A. Naphthalenediimide (NDI) Polymers for All-Polymer Photovoltaics. *Mater. Today* **2018**, *21*, 377−390.

(41) Liang, C.; Wang, H. Indacenodithiophene-Based D-A Conjugated Polymers for Application in Polymer Solar Cells. *Org. Electron.* **2017**, *50*, 443−457.

(42) Gao, C.; Wang, L.; Li, X.; Wang, H. Rational Design on D-A Conjugated P(BDT-DTBT) Polymers for Polymer Solar Cells. *Polym. Chem.* **2014**, *5*, 5200−5210.

(43) Cheng, P.; Li, G.; Zhan, X.; Yang, Y. Next-Generation Organic Photovoltaics Based on Non-Fullerene Acceptors. *Nat. Photonics 2018 123* **2018**, *12*, 131−142.

(44) Shao, Y.; Gan, Z.; Epifanovsky, E.; Gilbert, A. T. B.; Wormit, M.; Kussmann, J.; Lange, A. W.; Behn, A.; Deng, J.; Feng, X.; et al. Advances in Molecular Quantum Chemistry Contained in the Q-Chem 4 Program Package. *Mol. Phys.* **2015**, *113*, 184−215.

(45) Grimme, S. Accurate Description of van Der Waals Complexes by Density Functional Theory Including Empirical Corrections. *J. Comput. Chem.* **2004**, *25*, 1463−1473.

(46) Klimeš, J.; Michaelides, A. Perspective: Advances and Challenges in Treating van Der Waals Dispersion Forces in Density Functional Theory. *J. Chem. Phys.* **2012**, *137*, 120901.

(47) Jackson, N. E.; Kohlstedt, K. L.; Savoie, B. M.; Olvera de la Cruz, M.; Schatz, G. C.; Chen, L. X.; Ratner, M. A. Conformational Order in Aggregates of Conjugated Polymers. *J. Am. Chem. Soc.* **2015**, *137*, 6254−6262.

(48) Perkins, M. A.; Cline, L. M.; Tschumper, G. S. Torsional Profiles of Thiophene and Furan Oligomers: Probing the Effects of Heterogeneity and Chain Length. *J. Phys. Chem. A* **2021**, *125*, 6228−6237.

(49) Hoover, W. G. Canonical Dynamics: Equilibrium Phase-Space Distributions. *Phys. Rev. A* **1985**, *31*, 1695.

(50) Martínez, L.; Andrade, R.; Birgin, E. G.; Martínez, J. M. PACKMOL: A Package for Building Initial Configurations for Molecular Dynamics Simulations. *J. Comput. Chem.* **2009**, *30*, 2157−2164.

(51) Gedefaw, D.; Tessarolo, M.; Zhuang, W.; Kroon, R.; Wang, E.; Bolognesi, M.; Seri, M.; Muccini, M.; Andersson, M. R. Conjugated Polymers Based on Benzodithiophene and Fluorinated Quinoxaline for Bulk Heterojunction Solar Cells: Thiophene versus Thieno[3,2-b]Thiophene as π-Conjugated Spacers. *Polym. Chem.* **2014**, *5*, 2083−2093.

(52) Ning, L.; Han, G.; Yi, Y. Intra-Chain and Inter-Chain Synergistic Effect Gives Rise to High Electron Mobilities for Naphthalenediimide Based Copolymers. *J. Mater. Chem. C* **2020**, *8*, 16527−16532.

(53) Guo, X.; Kim, F. S.; Seger, M. J.; Jenekhe, S. A.; Watson, M. D. Naphthalene Diimide-Based Polymer Semiconductors: Synthesis, Structure-Property Correlations, and n-Channel and Ambipolar Field-Effect Transistors. *Chem. Mater.* **2012**, *24*, 1434−1442.